# Thin films of the spin ice compound Ho2Ti2O7

D. P. Leusink, F. Coneri, M. Hoek, S. Turner, H. Idrissi, G. Van Tendeloo, and H. Hilgenkamp

Citation: APL Materials **2**, 032101 (2014); doi: 10.1063/1.4867222
View online: http://dx.doi.org/10.1063/1.4867222
View Table of Contents: http://scitation.aip.org/content/aip/journal/aplmater/2/3?ver=pdfcov
Published by the AIP Publishing

# Thin films of the spin ice compound $Ho_2Ti_2O_7$

D. P. Leusink,[1] F. Coneri,[1] M. Hoek,[1] S. Turner,[2] H. Idrissi,[2,3]
G. Van Tendeloo,[2] and H. Hilgenkamp[1,a]
[1]*MESA+ Institute for Nanotechnology, University of Twente, P.O. Box 217, 7500 AE Enschede, The Netherlands*
[2]*Electron Microscopy for Materials Science (EMAT), Department of Physics, University of Antwerp, Groenenborgerlaan 171, B-2020 Antwerp, Belgium*
[3]*Institute of Mechanics, Materials and Civil Engineering, Université catholique de Louvain, Place Sainte Barbe 2, B-1348 Louvain-La-Neuve, Belgium*

(Received 20 December 2013; accepted 14 February 2014; published online 3 March 2014)

The pyrochlore compounds $Ho_2Ti_2O_7$ and $Dy_2Ti_2O_7$ show an exotic form of magnetism called the spin ice state, resulting from the interplay between geometrical frustration and ferromagnetic coupling. A fascinating feature of this state is the appearance of magnetic monopoles as emergent excitations above the degenerate ground state. Over the past years, strong effort has been devoted to the investigation of these monopoles and other properties of the spin ice state in bulk crystals. Here, we report the fabrication of $Ho_2Ti_2O_7$ thin films using pulsed laser deposition on yttria-stabilized $ZrO_2$ substrates. We investigated the structural properties of these films by X-ray diffraction, scanning transmission electron microscopy, and atomic force microscopy, and the magnetic properties by vibrating sample magnetometry at 2 K. The films not only show a high crystalline quality, but also exhibit the hallmarks of a spin ice: a pronounced magnetic anisotropy and an intermediate plateau in the magnetization along the [111] crystal direction.  [http://dx.doi.org/10.1063/1.4867222]

The magnetic $Ho^{3+}$ ions in $Ho_2Ti_2O_7$ form a lattice of corner-sharing tetrahedra in the pyrochlore structure and interact via ferromagnetic coupling.[1–7] Their magnetic moments are Ising-like due to the crystal field anisotropy and are aligned along the set of ⟨111⟩ axes. The resulting degenerate ground state of each tetrahedron has two holmium spins pointing inwards and two holmium spins pointing outwards. This is the so-called "ice rule," from the analogy with the H–O bond lengths in solid water. A local breaking of the ice rule, due to the flipping of one holmium spin shared between two neighboring tetrahedra, results in a 3-in-1-out and a 1-in-3-out configuration. This effectively creates a positive and a negative magnetic charge in the adjacent tetrahedra,[8] which can be regarded as a monopole-antimonopole pair.[9,10] Such pairs can dissociate and the individual monopoles can move away from each other by flipping a chain of spins along their route. This process takes place without further violating the ice rule, so that the energy cost for separating the monopoles to infinity stays finite, being linked to the energy required for the first excitation. Signatures of emergent magnetic monopoles in bulk spin ice crystals have been observed by several groups.[11–15] The magnetic counterparts of two fundamental effects in electronics have also been demonstrated: a basic capacitor effect for magnetic charges[16] and the introduction of magnetic defects hindering the monopole flow, similar to residual defect-induced resistance for electrons.[17] Further effort has been dedicated to tune the monopole chemical potential in a range where mutual interaction plays a role, to mimic electronic correlations in a purely magnetic Coulomb gas.[18] In conjunction with all the mentioned experiments, the term "magnetricity" is coined to describe the flow of magnetic

[a]Author to whom correspondence should be addressed. Electronic mail: h.hilgenkamp@utwente.nl.

 

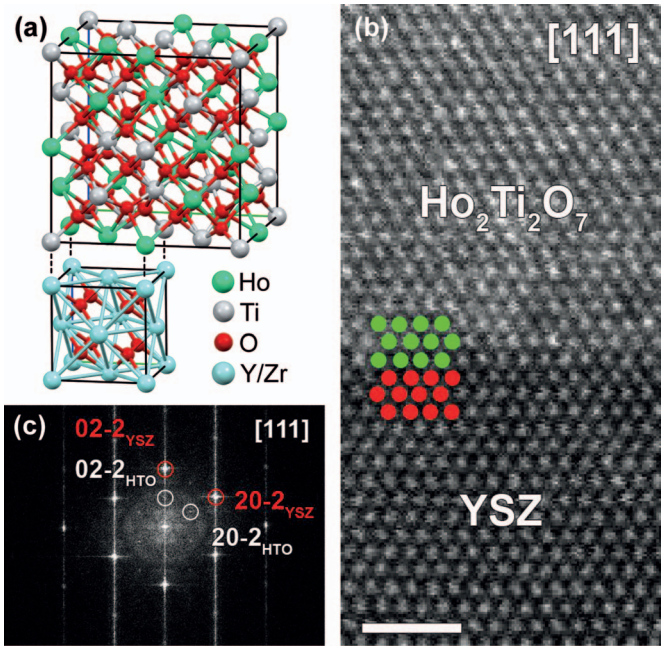


FIG. 1. (a) The pyrochlore structure of $Ho_2Ti_2O_7$ compared to the fluorite structure of YSZ. The lattice mismatch of $Ho_2Ti_2O_7$ with YSZ is 2%. (b) HAADF-STEM image of the (011)-oriented $Ho_2Ti_2O_7$/YSZ interface imaged along the [111] zone axis orientation. The Ho/Ti atomic columns in the $Ho_2Ti_2O_7$ layer are indicated by green dots, the Y/Zr atomic columns in the YSZ substrate by red dots. The indicated scale bar is 1 nm. (c) Fourier transform of the $Ho_2Ti_2O_7$ (HTO)/YSZ interface imaged along the [111] zone axis, evidencing the perfect epitaxial relationship of the layer with respect to the substrate.

charges as the equivalent of electricity. However, until now all experiments on spin ice materials have been performed on bulk crystals. A tantalizing prospect is to incorporate spin ice materials into devices for spintronics and devices that can manipulate the magnetic monopoles. This would require the availability of spin ice thin films. The possibility of making thin films will further advance the research into spin ice systems and the manipulation of the monopole states, and this study presents a crucial step towards the generation of real devices for "magnetronics."

We use pulsed laser deposition (PLD) to grow thin films of the spin ice material $Ho_2Ti_2O_7$ from a stoichiometric target. As substrates we use yttria-stabilized zirconia (YSZ) in the (001), (011), and (111) orientations. The lattice mismatch of YSZ with $Ho_2Ti_2O_7$ is 2% (Fig. 1(a)) and, prior to deposition, the YSZ substrates are annealed at 1050 °C to obtain a smooth surface. The growth rate is calibrated by X-ray reflectivity and cross-sectional scanning transmission electron microscopy (STEM), and the thickness of the deposited films is varied between 9 nm and 120 nm. High-angle annular dark field STEM (HAADF-STEM) studies reveal that the films are single crystalline (Fig. 1(b)) and epitaxially grown on YSZ (Fig. 1(c)).

The surface morphology of a (111)-oriented YSZ substrate prior to deposition, imaged by atomic force microscopy (AFM), is shown in Fig. 2(a). Terraces with steps of 3.1 ± 0.1 Å are observed, which corresponds to one third of the lattice constant of YSZ along the (111) direction. Even after deposition of a $Ho_2Ti_2O_7$ film of 110 nm, this terrace structure is still visible (Fig. 2(b)). Figure 2(c) shows an AFM image on a smaller scale. The typical peak-to-peak values of the films grown on differently oriented YSZ are between 1.5 and 5.5 nm and the root-mean-squared roughness of the films is between 0.4 and 1.2 nm. These low values indicate that the films are very smooth. Typical lateral dimensions for the growth islands are 20–40 nm, and STEM studies such as Fig. S1 in the supplementary material[19] show that crystallinity is preserved throughout the whole film thickness of 80 nm.

X-ray diffraction (XRD) is used to determine the quality of the crystal structure of the $Ho_2Ti_2O_7$ thin films. Fig. 3(a) shows symmetric $2\theta$-$\omega$ scans for ~110 nm $Ho_2Ti_2O_7$ films grown on differently oriented substrates. The presence of only out-of-plane peaks of $Ho_2Ti_2O_7$ further underlines the

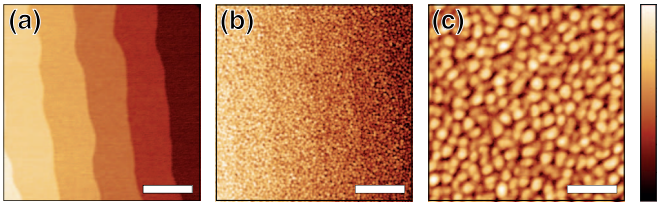


FIG. 2. (a) Image of (111)-oriented YSZ substrate prior to deposition. The step size corresponds to one third of the YSZ unit cell along the (111) direction. The indicated scale bar is 500 nm. (b) Image of a 110 nm $Ho_2Ti_2O_7$ film grown on the YSZ substrate shown in (a). The indicated scale bar is 500 nm. (c) Zoomed-in image of the $Ho_2Ti_2O_7$ film shown in (b). The indicated scale bar is 125 nm. The color scale on the right is between 0 and 7 nm and corresponds to the images in (b) and (c).

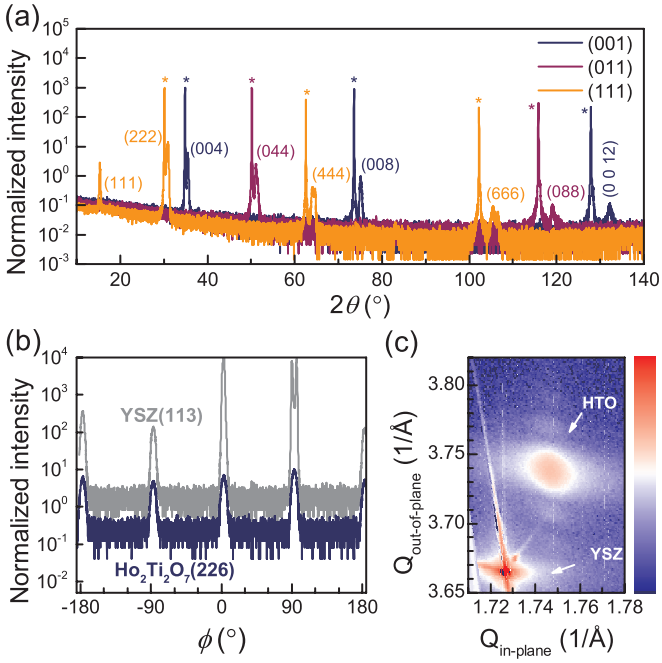


FIG. 3. (a) Symmetric $2\theta$-$\omega$ scans of 110 nm thick $Ho_2Ti_2O_7$ films grown on differently oriented YSZ substrates. The diffraction peaks marked with an asterisk originate from the substrate. (b) $\phi$ scan of the (226) diffraction peak of a 110 nm $Ho_2Ti_2O_7$ film compared to the (113) diffraction peak of the (001)-oriented YSZ substrate. The graphs are displaced vertically for clarity. (c) Reciprocal space map of the (226) diffraction peak of a 33 nm thick $Ho_2Ti_2O_7$ (HTO) film grown on a (001)-oriented YSZ substrate. The color scale is logarithmic and spans 5 decades.

high quality epitaxial growth of the films. From these diffraction peaks a lattice constant of 10.1 Å is obtained, corresponding with the expected stoichiometry. We note that a few samples have a lattice constant up to 10.2 Å. This could indicate an off-stoichiometry of the Ho and Ti ratio for those films,[20] possibly due to target inhomogeneity. The in-plane orientation of the crystal structure is investigated by performing $\phi$ scans around the (226) diffraction peak of $Ho_2Ti_2O_7$ (Fig. 3(b)). The expected four peaks, due to cubic symmetry, appear for the same $\phi$ angles as the (113) substrate diffraction peaks, confirming the cube-on-cube growth of the $Ho_2Ti_2O_7$ film on the substrate. Figure 3(c) shows the reciprocal space map of a 33 nm thick $Ho_2Ti_2O_7$ film. The (113) YSZ and the (226) $Ho_2Ti_2O_7$ diffraction peaks appear at different in-plane values of the scattering vector $\boldsymbol{Q}$. The film is therefore mainly relaxed and not fully strained to the substrate. This is expected for such a large thickness, but films with a thickness of 9 nm also show relaxation. This suggests that the elasticity of the crystal structure of $Ho_2Ti_2O_7$ is low. The presence of Kiessig fringes in Fig. 3(c) also underlines the smoothness of the grown film.

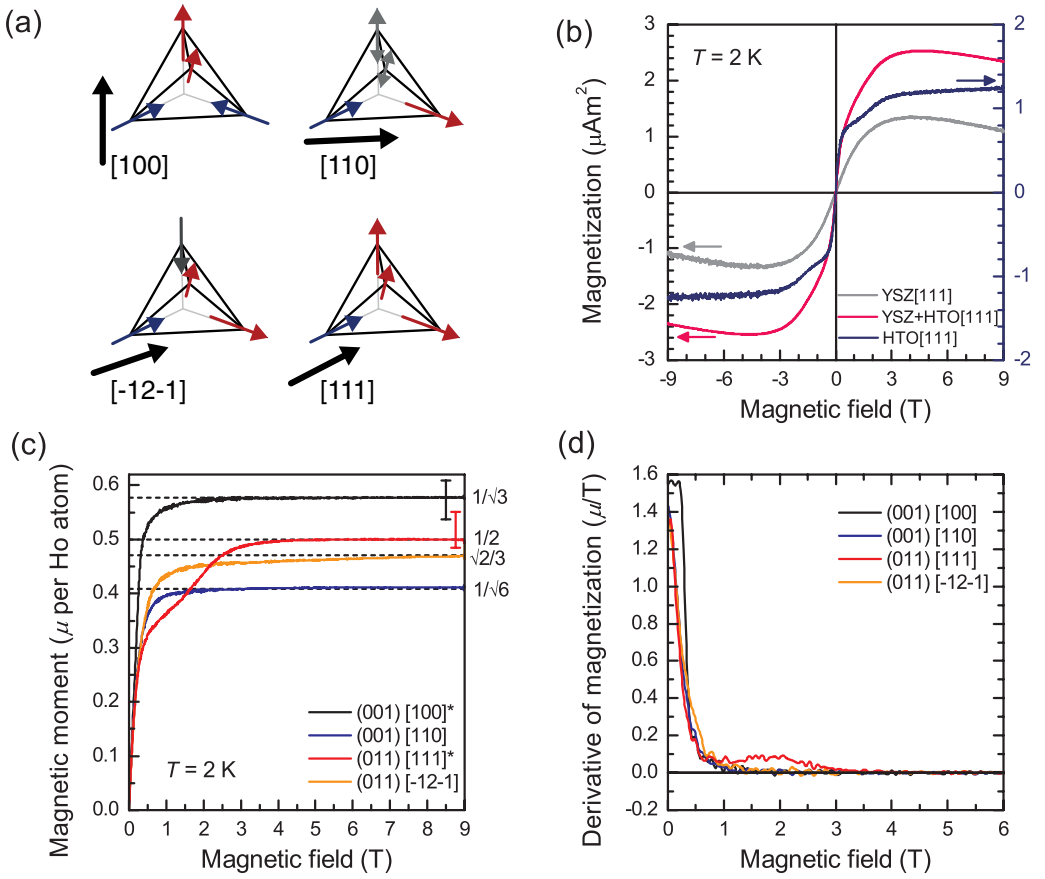


FIG. 4. (a) The investigated field directions (black arrows) compared to the orientation of the holmium spins on a tetrahedron. The gray holmium spins do not contribute to the magnetization, as their orientation is perpendicular to the field. The blue spins point inwards the tetrahedron and the red spins outwards. (b) Magnetization along the [111] direction for an 80 nm $Ho_2Ti_2O_7$ film grown on (011)-oriented YSZ. The gray curve shows the magnetization of the substrate, the pink curve is the magnetization of the total sample, and the blue curve is their difference, corresponding to the magnetization of only the $Ho_2Ti_2O_7$ film. Note that the scale of the blue curve is given by the right axis. (c) Magnetization of 110–120 nm $Ho_2Ti_2O_7$ films as function of applied field along different crystal orientations showing the magnetic anisotropy. Units of the magnetization are in averaged magnetic moment per holmium atom $\mu$. The dotted lines indicate the theoretical values for the saturation magnetizations. The saturation magnetizations of the [100] direction and the [111] direction (indicated by an asterisk in the legend) are scaled to their expected values. The magnetizations of the [110] and the $[\bar{1}2\bar{1}]$ directions are scaled relative to the [100] and [111] directions, respectively. The error bars on the [100] and [111] curves indicate the possible spread in saturation magnetization caused by the sample specific uncertainties, which are eliminated due to the scaling to the expected values. For more details on the uncertainties, see the supplementary material.[19] (d) First derivative of the magnetization curves shown in (c).

Although the studies on the crystal structure confirm the high quality of the $Ho_2Ti_2O_7$ films, the most important question is whether these films also show the spin ice behavior. The spin ice model with the corresponding ice rules predicts that spin ice materials should exhibit magnetic anisotropy and the presence of an intermediate state in the magnetization along the [111] crystal orientation.[21] These features have been measured in single crystals of $Ho_2Ti_2O_7$[22,23] and $Dy_2Ti_2O_7$.[24] To verify whether our $Ho_2Ti_2O_7$ thin films also show these characteristics, the magnetic properties of films with a thickness in the range of 80–120 nm were studied by vibrating sample magnetometry (VSM). We investigated $Ho_2Ti_2O_7$ films grown on differently oriented substrates to determine the in-plane magnetization for different crystal orientations of $Ho_2Ti_2O_7$. The investigated field directions are shown in Fig. 4(a). The pink curve in Fig. 4(b) shows the field dependence of the magnetization for a 110 nm $Ho_2Ti_2O_7$ film grown on a (011)-oriented substrate and measured along the [111] direction at a temperature of 2 K, which is near the onset of the spin correlations.[22] This curve is obtained by

subtracting the magnetization originating from the substrate (gray curve) prior to deposition from the total magnetization, caused by the $Ho_2Ti_2O_7$ film and the substrate (blue curve). The absence of ferromagnetic hysteresis is expected due to the frustration in spin ice materials and the fact that the temperature of this measurement is above the spin freezing temperature of ∼0.7 K.[3–5,25] These observations are similar for all films grown on differently oriented YSZ substrates. The remarkable difference between the [111] direction and the other directions is the observation of the intermediate plateau at about 1.5 T. This is a hallmark of the spin ice behavior: for small magnetic fields applied along the [111] direction, one of the holmium spins in the tetrahedron is not aligned along this field due to the ice rule. The step-like enhancement of the magnetization appears when this spin aligns with the magnetic field and thus with breaking of the ice rule.

To verify whether, besides this distinct feature for spin ice behavior, the expected magnetic anisotropy is also present in these thin films, we compare the saturation magnetizations along different crystal directions. The magnetic moment per holmium atom can be extracted from a magnetization curve as presented in Fig. 4(b). Although the obtained values are of the correct order, there is too much scatter in the values between different samples to quantitatively compare the experimental results with the theory. This error is caused by uncertainties related to the sample and the VSM measurement itself.[19] To exclude the sample specific uncertainties, the sample has been rotated on the sample holder for the VSM, so that in one sample the magnetization along different in-plane orientations can be measured. Two types of samples were measured: a (001)-oriented sample and a (011)-oriented sample. The measured in-plane orientations are the [100] and [110] orientations for the (001)-oriented sample, and the [111] and $[\bar{1}2\bar{1}]$ directions for the (011)-oriented sample (Fig. 4(c)). The expected averaged magnetizations per holmium atom are $\mu/\sqrt{3}$ for the [100] orientation, $\mu/2$ for the [111] orientation, $\mu/\sqrt{6}$ for the [110] orientation, and $\mu\sqrt{2}/3$ for the $[\bar{1}2\bar{1}]$ orientation, where $\mu$ is the total moment of $10\mu_B$ for one holmium spin.[21] These values are indicated in Fig. 4(c) by dashed lines. To relate the strength of the measured magnetic signals to the film thickness, we scale the measurements on the (001)-oriented sample relative to the expected value of the strongest signal, namely, along the [100] direction. The same is done for the (011)-oriented sample: as the [111] direction gives the stronger signal compared to the $[\bar{1}2\bar{1}]$ direction, the measured magnetic signals are scaled to the expected value of the [111] direction. These orientations are indicated by an asterisk in the legend of Fig. 4(c). The sample specific uncertainties are removed due to this scaling method. The error bars on the [100] and [111] magnetization curves give the possible spread in magnetic moment per holmium atom caused by these sample specific uncertainties. As the scaled saturation magnetizations fall within these thickness ranges, we conclude that the film thicknesses extracted from these scaled measurements correspond to the estimated thicknesses of 110–120 nm, as derived from the number of PLD pulses (see the supplementary material for more information[19]).

The anisotropy due to the crystal field is clearly visible in Fig. 4(c) and the saturations along the [110] and $[\bar{1}2\bar{1}]$ directions approach the expected relative ratio values of the spin ice model. The magnetizations of the [100] and [110] orientations saturate at ∼3 T and the magnetization of the [111] orientation at ∼5 T due to the intermediate state at lower magnetic fields. By contrast, the magnetization along the $[\bar{1}2\bar{1}]$ direction does not saturate in the measured magnetic field range. Figure 4(d) shows the derivative of the magnetization to the magnetic field. The curve of the [100] direction behaves differently from the other curves for fields lower than ∼1 T, where the sharp transition to saturation indicates the cooperative phase transition expected for the [100] direction.[21] For fields higher than ∼1 T only the curve of the [111] direction behaves differently due to the intermediate state at ∼1.5 T. From Fig. 4(d) it appears that the magnetization for the $[\bar{1}2\bar{1}]$ direction is also saturated at 3 T, like the magnetizations for the [100] and [110] directions. The ratio between the magnetizations of the [100] and [110] directions $M_{[100]}/M_{[110]}$ deviates with −0.3% from the expected ratio of $\sqrt{2}$ at 3 T and with −0.7% at 9 T. This could mean that the magnetization of the [110] direction is larger than expected. A similar observation on a $Dy_2Ti_2O_7$ crystal[24] was explained by the magnetic anisotropy with a slight misalignment during the VSM measurement and the same argument can be applied to the $Ho_2Ti_2O_7$ thin films (see the supplementary material for calculations of uncertainties due to a misalignment[19]). The ratio at lower magnetic fields for the (011)-oriented sample $M_{[111]}(3T)/M_{[\bar{1}2\bar{1}]}(5T)$ deviates with 3% from the expected ratio of $3/(2\sqrt{2})$, while at 9 T

this deviation has decreased to 0.4% due to the apparent non-saturation of the $[\bar{1}2\bar{1}]$ direction. While this deviation is small, it probably cannot be explained by only a misalignment. In case of a slight misalignment we would have measured a larger magnetization for the $[\bar{1}2\bar{1}]$ direction or a smaller magnetization for the [111] direction.[19] Instead, the measured magnetization for the [111] direction is too large or the measured magnetization for the $[\bar{1}2\bar{1}]$ direction is too small compared to the spin ice model. Other possibilities for a different magnetization could be edge effects, due to the large surface-bulk ratio in thin films, or defects. Other factors related to the experimental setup[19] could already result in a deviation of a few percent. However, the magnetic anisotropy is clearly visible from the curves shown in Fig. 4(c) and combining this with the observation of the plateau in the magnetization curve for the [111] direction, we conclude that the $Ho_2Ti_2O_7$ films grown by PLD exhibit spin ice behavior.

In this study we have demonstrated the single crystalline thin film growth of the spin ice compound $Ho_2Ti_2O_7$, showing the spin ice behavior. The magnetic behavior of the thin films presented here is very similar to the behavior of bulk single crystals.[22,23] The ability to grow spin ice thin films opens up new research directions on the spin ice dynamics in these frustrated systems. Questions about the influence of dimension reduction can be addressed by growing ultrathin films. If the growth conditions are optimized for layer-by-layer growth using *in situ* reflective high-energy electron diffraction, even films with a thickness of 1 unit cell are feasible. Using bicrystal substrates, grains with different crystal orientations could be induced, allowing detailed studying the influence of grain boundaries on the spin ice behavior. The availability of thin films enables to structure the spin ice material into devices and combine it with other materials by patterning on the micro- and nanoscale, e.g., to manipulate the monopoles via their electric dipoles using electrical gating.[26] The spin ice material itself can be easily modified by varying target composition or deposition conditions, or by post-annealing. This, and epitaxial strain engineering, may allow changing the chemical potential and the density of monopoles to enter the regime of monopole correlations.[18] We notice that also other pyrochlore oxides show, or are predicted to show, interesting properties. An example is $Y_2Ir_2O_7$, which is suggested to be a topological Mott insulator.[27] Also for those materials, the development of thin film growth will be of great interest, which may be stimulated by the example of $Ho_2Ti_2O_7$ presented here.

After submission of our manuscript, we became aware that in a parallel effort to our research, also $Dy_2Ti_2O_7$ films have been realized.[28]

The authors acknowledge support from the Dutch FOM and NWO foundations and from the European Union under the Framework 7 program under a contract from an Integrated Infrastructure Initiative (Reference 312483 ESTEEM2). G.V.T. acknowledges the ERC Grant N246791-COUNTATOMS. S.T. gratefully acknowledges financial support from the Fund for Scientific Research Flanders (FWO). H.I. acknowledges the IAP program of the Belgian State Federal Office for Scientific, Technical and Cultural Affairs under Contract No. P7/21. The microscope used in this study was partially financed by the Hercules Foundation of the Flemish Government. The authors acknowledge fruitful interactions with A. Brinkman, M. G. Blamire, M. Egilmez, F. J. G. Roesthuis, J. N. Beukers, C. G. Molenaar, M. Veldhorst, and X. Renshaw Wang.

[1] M. J. Harris, S. T. Bramwell, D. F. McMorrow, T. Zeiske, and K. W. Godfrey, Phys. Rev. Lett. **79**, 2554 (1997).
[2] A. P. Ramirez, A. Hayashi, R. J. Cava, R. Siddharthan, and B. S. Shastry, Nature (London) **399**, 333–335 (1999).
[3] S. T. Bramwell, M. J. Harris, B. C. den Hertog, M. J. P. Gingras, J. S. Gardner, D. F. McMorrow, A. R. Wildes, A. L. Cornelius, J. D. M. Champion, R. G. Melko, and T. Fennel, Phys. Rev. Lett. **87**, 047205 (2001).
[4] S. T. Bramwell and M. J. P. Gingras, Science **294**, 1495–1501 (2001).
[5] R. Siddharthan, B. S. Shastry, A. P. Ramirez, A. Hayashi, R. J. Cava, and R. Rosenkranz, Phys. Rev. Lett. **83**, 1854–1857 (1999).
[6] B. C. den Hertog and M. J. P. Gingras, Phys. Rev. Lett. **84**, 3430–3433 (2000).
[7] S. V. Isakov, R. Moessner, and S. L. Sondhi, Phys. Rev. Lett. **95**, 217201 (2005).
[8] I. A. Ryzhkin, J. Exp. Theor. Phys. **101**, 481–486 (2005).
[9] C. Castelnovo, R. Moessner, and S. L. Sondhi, Nature (London) **451**, 42–45 (2008).
[10] C. Castelnovo, R. Moessner, and S. L. Sondhi, Annu. Rev. Condens. Matter Phys. **3**, 35–55 (2012).
[11] L. D. C. Jaubert and P. C. W. Holdsworth, Nature Phys. **5**, 258–261 (2009).

[12] D. J. P. Morris, D. A. Tennant, S. A. Grigera, B. Klemke, C. Castelnovo, R. Moessner, C. Czternasty, M. Meissner, K. C. Rule, J.-U. Hoffmann, K. Kiefer, S. Gerischer, D. Slobinsky, and R. S. Perry, Science **326**, 411–414 (2009).
[13] T. Fennell, P. P. Deen, A. R. Wildes, K. Schmalzl, D. Prabhakaran, A. T. Boothroyd, R. J. Aldus, D. F. McMorrow, and S. T. Bramwell, Science **326**, 415–417 (2009).
[14] H. Kadowaki, N. Doi, Y. Aoki, Y. Tabata, T. J. Sato, J. W. Lynn, K. Matsuhira, and Z. Hiroi, J. Phys. Soc. Jpn. **78**, 103706 (2009).
[15] S. T. Bramwell, S. R. Giblin, S. Calder, R. Aldus, D. Prabhakaran, and T. Fennel, Nature (London) **461**, 956–959 (2009).
[16] S. R. Giblin, S. T. Bramwell, P. C. W. Holdsworth, D. Prabhakaran, and I. Terry, Nature Phys. **7**, 252–258 (2011).
[17] H. M. Revell, L. R. Yaraskavitch, J. D. Mason, K. A. Ross, H. M. L. Noad, H. A. Dabkowska, B. D. Gaulin, P. Henelius, and J. B. Kycia, Nature Phys. **9**, 34–37 (2013).
[18] H. D. Zhou, S. T. Bramwell, J. G. Cheng, C. R. Wiebe, G. Li, L. Balicas, J. A. Bloxsom, H. J. Silverstein, J. S. Zhou, J. B. Goodenough, and J. S. Gardner, Nat. Commun. **2**, 478 (2011).
[19] See supplementary material at http://dx.doi.org/10.1063/1.4867222 for the fabrication procedure, experimental methods, a discussion of factors influencing the measured magnetization, and for more details on the uncertainty bars shown in Fig. 4(c).
[20] G. C. Lau, B. D. Muegge, T. M. McQueen, E. L. Duncan, and R. J. Cava, J. Solid State Chem. **179**, 3126–3135 (2006).
[21] M. J. Harris, S. T. Bramwell, P. C. W. Holdsworth, and J. D. M. Champion, Phys. Rev. Lett. **81**, 4496 (1998).
[22] A. L. Cornelius and J. S. Gardner, Phys. Rev. B **64**, 060406 (2001).
[23] O. A. Petrenko, M. R. Lees, and G. Balakrishnan, Phys. Rev. B **68**, 012406 (2003).
[24] H. Fukazawa, R. G. Melko, R. Higashinaka, Y. Maeno, and M. J. P. Gingras, Phys. Rev. B **65**, 054410 (2002).
[25] K. Matsuhira, Y. Hinatsu, K. Tenya, and T. Sakakibara, J. Phys.: Condens. Matter **12**, L649–L656 (2000).
[26] D. I. Khomskii, Nat. Commun. **3**, 904 (2012).
[27] D. Pesin and L. Balents, Nature Phys. **6**, 376–381 (2010).
[28] S. T. Bramwell *et al.*, private communication (2014).